# Fracture Phase Separation

Takehito Koyama, Takeaki Araki, and Hajime Tanaka*

*Institute of Industrial Science, University of Tokyo, Meguro-ku, Tokyo 153-8505, Japan*

(Received 29 September 2008; revised manuscript received 3 December 2008; published 10 February 2009)

Here we report novel phase-separation behavior accompanying mechanical fracture (''fracture phase separation''), which is observed in polymer solutions. Surprisingly, mechanical fracture becomes a dominant coarsening process of the phase separation. The transition from viscoelastic to fracture phase separation corresponds to the ''ductile-to-brittle transition'' in fracture of materials under shear deformation. The only difference between fracture phase separation and material fracture is whether the deformation is induced internally by phase separation itself or externally by loading. This suggests a general physical scenario of mechanical selection of the kinetic pathway of inhomogeneization of materials under stress.

DOI: 10.1103/PhysRevLett.102.065701 PACS numbers: 64.75.Va, 05.70.Fh, 62.20.M−, 83.80.Rs

Phase-separation phenomena are widely observed in various kinds of condensed matter including metals, semiconductors, oxides, simple liquids, and complex fluids such as polymers, surfactants, colloids, emulsions, geomaterials, and biological materials [1–3]. The phenomena lead to pattern evolution in multicomponent mixtures of these materials and thus play key roles in their morphological control, which is related to various functions associated with mechanical, electric, and transport properties. Phase separation had been classified into solid and fluid models [1,2]. Solid phase separation can be seen in phase separation of metallic alloys, whereas fluid phase separation can be seen, e.g., in phase separation of salad dressing into the oil-rich and water-rich phases.

Nearly 20 years ago, however, we found a novel type of phase-separation behavior in polymer solutions [4,5], which can be explained by neither of these models. In addition to the initial diffusive and the final hydrodynamic regimes which are known for classical phase separation, there exists an intermediate viscoelastic regime, where elastic force balance determines domain morphology instead of interface tension. Contrary to the common sense of classical phase separation, even the minority phase transiently forms a continuous network structure. The process of this phase separation is characterized by a crossover between the characteristic deformation rate and the characteristic rheological relaxation rate, which can be viewed as viscoelastic relaxation for pattern evolution. Thus, it was named ''viscoelastic phase separation (VPS)'' [4,6]. The key to VPS is dynamic asymmetry between the two components of a mixture. In a polymer solution, for example, because polymers are much larger than the surrounding solvent molecules, they move much more slowly. This dynamic asymmetry means the small, fast molecules can relax on time scales many orders of magnitudes faster than the large, slow particles. Such ''dynamic asymmetry'' can be induced by either the large size difference or the difference in a glass-transition temperature between the components of a mixture [5,6].

Here we report novel phase-separation behavior accompanying fracture in polymer solutions, which is different from any of the known phase-separation behaviors. Samples used were mixtures of monodisperse polystyrene (PS) and diethyl malonate (DEM). The weight-averaged molecular weights of PS ($M_w$) were $7.04 \times 10^5$ (PS1) and $3.84 \times 10^6$ (PS2). $M_w/M_n$ ($M_n$: number-averaged molecular weight) is 1.05 for PS1 and 1.04 for PS2. These mixtures have upper-critical-solution-temperature (UCST) type phase diagrams [7]. The critical composition $\phi_c$ and temperature $T_c$ are determined as 4.89 wt% and 21.5 °C for a PS1/DEM mixture and as 2.14 wt% and 27.2 °C for a PS2/DEM mixture. The polymer solutions were sandwiched between two cover glasses, whose spacing was set to be 5 $\mu$m by using monodisperse glass beads. Then they were placed on a temperature-controlled hot stage (Linkam, LK-600PH). After a temperature quench, the pattern evolution was observed with phase-contrast microscopy (Olympus, BH-2).

When we quench a polymer solution near $\phi_c$ shallowly to avoid the formation of a transient gel, fluidlike phase separation with bicontinuous morphology takes place (region E in Fig. 1). If we quench the same system deeply enough to create a transient gel state, VPS takes place (region D in Fig. 1). Near $\phi_c$, VPS is characterized by (i) the formation of a transient gel, (ii) nucleation of solvent-rich holes in it, (iii) the subsequent network formation of the polymer-rich phase (transient gel) (Fig. 1), and (iv) viscoelastic relaxation of the network pattern to isolated domains. This process accompanies phase inversion, namely, the initially majority polymer-rich phase eventually becomes the minority phase [Fig. 2(a)]. What surprises us is that a further deeper quench leads to mechanical fracture of a transient gel [Fig. 2(b); see also Fig. 3]. In other words, fracture becomes the dominant coarsening mechanism of phase separation. Thus, we call this novel type of phase separation ''fracture phase separation (FPS).'' A transient gel tends to shrink, but the connectivity does not allow uniform shrinkage. As the

 

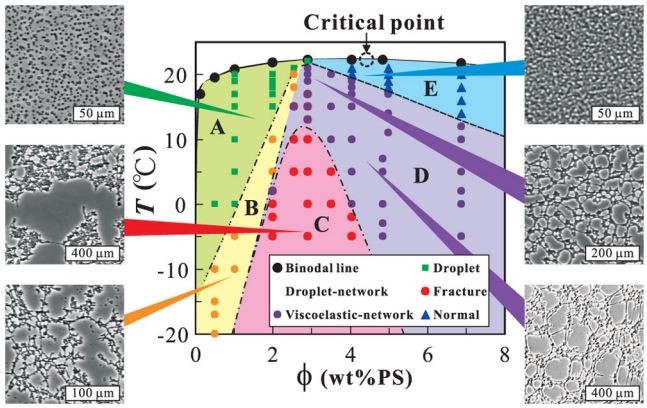


FIG. 1 (color online). Kinetic phase diagram and typical phase-separation patterns observed in PS1/DEM mixtures. In region A, normal fluid phase separation takes place. The polymer-rich phase appears as droplets. In region B, polymer-rich droplets are initially formed, but they form a percolated network. After the percolation, the morphology is determined by mechanical force balance. In region C, novel FPS is observed. In region D, typical VPS is observed. After the formation of a transient gel, the minority polymer-rich phase forms a network structure. In region E, normal phase separation takes place. The solvent-rich phase appears as droplets there. The boundaries of region C are dependent upon the cell thickness, which is characteristic of elastic instability.

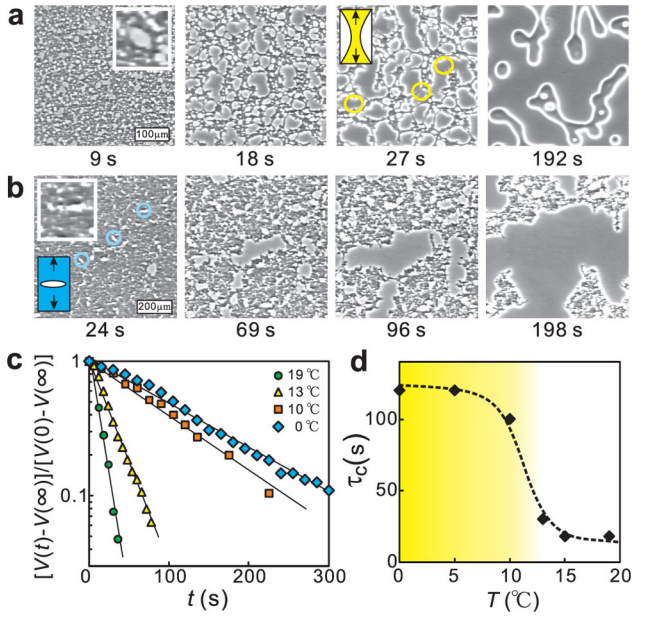


FIG. 2 (color online). Pattern evolution observed in a PS1/DEM mixture (2.91 wt % PS). (a) VPS observed after a quench to 15 °C. (b) FPS observed after a quench to 0 °C. In the yellow circles in (a), we can see that the polymer-rich phase is elongated under the stretching force generated by its volume shrinking (see also the small schematic figure). This resembles a typical ductile fracture of material under elongational deformation. In the blue circles in (b), on the other hand, we can see that the polymer-rich phase is fractured under the stretching force generated by its volume shrinking (see also the small schematic figure). This resembles a typical brittle fracture of material under elongational deformation. (c) Volume shrinking kinetics. (d) The characteristic time of the volume shrinking $\tau_c$ as a function of the quenched temperature $T$. There is a sharp increase in $\tau_c$ reflecting a transition from VPS to FPS. The small images with white edges are enlarged by 5 × .

result, the self-generated stress eventually leads to crack formation. These cracks grow with time as in the usual fracture process. This feature can be clearly seen in the low-magnification observation of FPS (Fig. 3).

There exists a transition from VPS to FPS with an increase in the quench depth. The transition is recognized not only from the characteristics of pattern evolution [Figs. 2(a) and 2(b)], but also from the volume (area) shrinking kinetics of the polymer-rich phase [Figs. 2(c) and 2(d)]. Figure 2(c) shows the volume shrinking dynamics during phase separation: $[V(t) - V(\infty)]/[V(0) - V(\infty)]$ is plotted against the phase-separation time $t$. Here $V(t)$ is the volume (area) fraction of the polymer-rich phase at time $t$, which is estimated by a black and white operation for images. See also the supplementary movie [8]. We found the relation $[V(t) - V(\infty)]/[V(0) - V(\infty)] = \exp(-t/\tau_c)$ for both VPS [5,6] and FPS (see the fitted straight lines). The temperature dependence of $\tau_c$ is plotted in Fig. 2(d), which shows that there is a change of the rheological response of the polymer-rich phase from viscoelastic to solidlike behavior. For FPS, solidlike fracture is the only process of volume (stress) relaxation of the polymer-rich phase, whereas for VPS continuous viscoelastic relaxation can induce the fast relaxation. This may be an origin of the behavior of $\tau_c$. Using these fingerprints, we constructed the dynamic phase diagram (Fig. 1), which tells us the type of phase separation occurring at each state point.

In a dynamically asymmetric mixture (e.g., polymer solution), a transient gel state may appear as a consequence of a dynamic crossover between the volume deformation rate and the rheological relaxation rate. The formation of such a transient gel is the origin of VPS [6,7]. The interaction network of the fast component (solvent) can relax to its lowest energy state very quickly, while that of the slow component (polymer) cannot. This is because the connectivity of the interaction network prevents the slow component from forming a compact structure having a lower energy. This effect of connectivity can be described by the bulk stress, which acts against the volume deformation of the transient gel (the polymer network) [6]. For the phase separation to proceed, the breakup of the network is required. The key feature of a transient gel is that it stores elastic energy that is created by the driving force of phase separation itself. In this regime, the domain shape is determined by the elastic force balance.

Now we discuss the physical mechanism of FPS. As described above, VPS is the process of fracture of a transient gel under volume deformation. We argue that FPS is the process of mechanical fracture of a transient gel against self-generated shear deformation. For slow shear deformation, a transient gel behaves as viscoelastic matter and

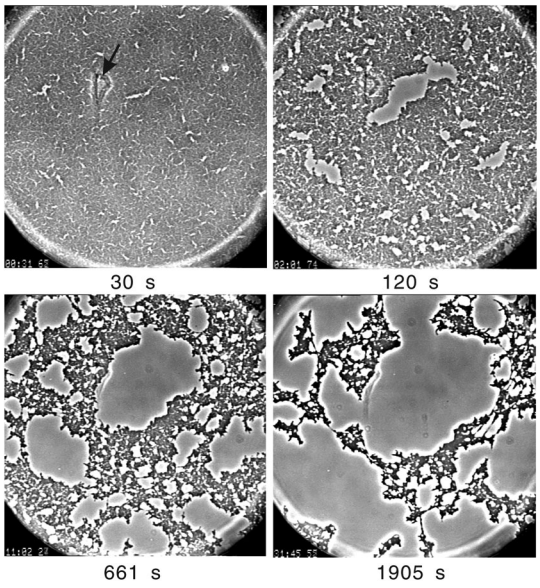


FIG. 3. FPS observed at a low magnification for a PS2/DEM mixture (4 wt% PS) after a quench to 22 °C. Formation and growth of cracks are clearly observed. The temporal increase in the contrast means the increase of $\phi$ in the transient gel. The diameter of the circular window is 1 mm. The object indicated by the arrow (30 s) is a crack on the glass window of the hot stage. Since it is located outside the sample, it does not affect the phenomena. See also the supplementary movie [8].

exhibits ductile fracture behavior for shear deformation: viscoelastic phase separation. The network is stretched continuously under stress, elongated, and eventually breaks up [Fig. 2(a)]. This process resembles a material undergoing ductile fracture under a stretching force [9–12]. For fast shear deformation, a transient gel should behave as a solid and exhibit brittle fracture behavior: fracture phase separation. This brittle fracture behavior is a manifestation of the solidlike behavior [11,12] of the transient gel. This scenario of mechanical instability is basically the same as shear-induced cavitation in a viscous liquid: self-amplification of density fluctuations under shear [13]. The instability of the interaction network for the volume deformation of type $\vec{\nabla} \cdot \vec{v}_p < 0$ ($\vec{v}_p$: polymer velocity) is a consequence of a steep composition dependence of the bulk stress, which we approximate as $G_B = G_B^0 \Theta(\phi - \phi_0^B)$, where $\Theta$ is a step function and $\phi_0^B$ is the threshold polymer composition for the bulk modulus [14]. On the other hand, we propose that a steep composition dependence of the shear modulus $G_S$ leads to its instability for shear-type deformation, which should be the origin of fracturelike behavior. To mimic this, we introduce a steplike composition dependence of $G_S(\phi)$: $G_S(\phi) = G_S^0 \Theta(\phi - \phi_0^S)$, where $\phi_0^S$ is the threshold polymer composition for the shear modulus. For the regime of FPS, the breakup of bonds is required not only for volume deformation, but also shear deformation of the network. To confirm this physical picture, we performed numerical simulations using the above $\phi$-dependent bulk and shear modulus on the basis of a two-fluid model, using basically the same equations as in [14] except for the functional form of $G_S(\phi)$ (see supplementary information [8]). The results are shown in Fig. 4. The simulations capture all the essential features of VPS and FPS, which supports the relevance of our physical picture.

Next we consider the location of the transition between VPS and FPS (Fig. 1) on a qualitative level. The $T$ dependence may be explained by the fact that both the number density and lifetime of crosslinking points in a transient gel increase with decreasing $T$. So the shear relaxation time increases with decreasing $T$. On the other hand, the characteristic time of volume deformation decreases. The crossover of these time scales may explain the $T$ dependence of the transition. For the $\phi$ dependence, the characteristic deformation rate is determined by the degree of the volume shrinking after the formation of a transient gel, which decreases for both very high and very low $\phi$. With an increase in $\phi$, the degree of the volume change from the initial transient gel (initially, almost 100%) to the final volume fraction of the polymer-rich phase becomes smaller. With a decrease in $\phi$, on the other hand, a continuous transient gel state becomes harder to be formed. In region B, the network is formed by a different mechanism: The polymer-rich droplets are formed first, and then aggregate to form a network [15].

Here it may be worth discussing the relationship between mechanical phase separation and fracture of materials. It is well established that a material under shear deformation (shear rate $\dot{\gamma}$) flows as liquid for $\dot{\gamma}\tau \ll 1$, behaves as viscoelastic matter for $\dot{\gamma}\tau \sim 1$, and as elastic body for $\dot{\gamma}\tau \gg 1$ [16,17]. Here $\tau$ is the terminal relaxation time of a material. Similarly, VPS is a result of a crossover of $\dot{\gamma}$ characterizing the deformation rate accompanied by

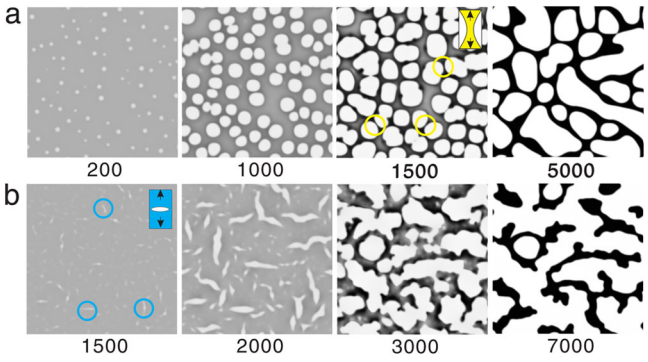


FIG. 4 (color online). Pattern evolution kinetics of VPS and FPS simulated by our model [14]. (a) VPS. Here $\phi_0 = 0.35$, $G_B = 5\theta(\phi - 0.35)$, $G_S = 0.5\phi^2$, and $\tau_B = \tau_S = 50\phi^2$. (b) FPS. Here $\phi_0 = 0.35$, $G_B = 5\theta(\phi - 0.35)$, $G_S = 5\theta(\phi - 0.33)$, and $\tau_B = \tau_S = 50\phi^2$, which are the bulk and shear relaxation times [14]. The anisotropic solvent holes appear due to the strongly nonlinear shear modulus. This captures the characteristic features of FPS observed experimentally. Compare these with Figs. 2(a) and 2(b) (for which the same annotation was used).

TABLE I. Classification of mechanical fracture and phase separation. Here "volume" means volume (bulk) deformation and "shear" means shear deformation.

| Material classification | Type of shear-induced fracture | Type of phase separation | Characteristics |
|---|---|---|---|
| liquid matter | cavitation | liquid phase separation | no fracture |
| viscoelastic matter | ductile fracture | viscoelastic phase separation | brittle (volume); ductile (shear) |
| solid matter | brittle fracture | fracture phase separation | brittle (both volume and shear) |

phase separation itself with $1/\tau$ of the polymer-rich phase. Solidlike mechanical fracture takes place when the strain exceeds a critical value in the elastic regime ($\dot{\gamma}\tau \gg 1$). FPS is the result of such large shear deformation over the mechanical stability limit. The key to these phenomena is that deformation couples with composition ($\phi$) [3] or density ($\rho$) fluctuations [13], which leads to a positive feedback toward mechanical instability through the fact that the lowering of $\phi$ or $\rho$ induces the shortening of $\tau$ and/or the decrease of the shear modulus $G$. Our study establishes a one-to-one relationship between mechanical behavior of materials under deformation and phase-separation behavior (Table I). Here we revealed that there are four types of phase separation in nature: solid, fluid, viscoelastic, and fracture phase separation. For the latter three types, which can be regarded as special cases of VPS, the momentum conservation, or the force balance condition, selects the kinetic pathway of pattern evolution together with a constitutive equation describing the rheological behavior of the material. We emphasize that this physical principle of the selection of the kinetic pathway is common to both phase separation and rheology. This forms an interesting analogy of mechanical behavior of material to phase separation (Table I). Mechanical fracture may be viewed as a special case of strain-induced phase separation: strain-induced inhomogeneization of the density field.

Finally, we consider the generality of FPS. It has been established that VPS is universally observed in various types of dynamically asymmetric mixtures [6]. This suggest that FPS, which is a special case of VPS, may also be observed in any dynamically asymmetric mixtures for $\dot{\gamma}\tau \gg 1$. For example, mechanical instability of actin gels (active cytoskeltal networks) driven by forces generated by motor proteins may be such an example [18,19] (see, e.g., Fig. [1c] in [19]). We note that for a crosslinked actin gel, the fracture should always be brittle-type since the rheological relaxation time of the gel should almost be infinite. Furthermore, FPS has similarity to other types of pattern formation induced by mechanical instability, such as shrinkage-crack formation. Formation of shrinkage-crack patterns is an ubiquitous phenomenon that is commonly observed in both nature (tectonic plates, dried mud layers, and cracks on rocks) and materials (concrete, ceramic glaze, glass, and coatings) [20]. They appear in materials which contract upon cooling or drying: mechanical instability associated with volume (area) shrinking. Thus, such crack formation should share the common physical mechanism with FPS. We note that the early stage of fracture phase separation [see, e.g., Fig. 3 ($t = 30$ s)] is striking similar to typical shrinkage-crack patterns. Thus, fracture phase separation may provide a general perspective on the mechanical instability of materials upon shrinking, or self-induced mechanical fracture.

The authors thank David A. Head for a critical reading of our manuscript. This work was partially supported by a grant-in-aid from the MEXT, Japan .

*tanaka@iis.u-tokyo.ac.jp

[1] P. C. Hohenberg and B. I. Halperin, Rev. Mod. Phys. **49**, 435 (1977).
[2] J. D. Gunton, M. San Miguel, and P. Sahni, *Phase Transition and Critical Phenomena* (Academic, London, 1983), Vol. 8.
[3] A. Onuki, *Phase Transition Dynamics* (Cambridge University Press, Cambridge, England, 2002).
[4] H. Tanaka, Phys. Rev. Lett. **71**, 3158 (1993).
[5] H. Tanaka, Phys. Rev. Lett. **76**, 787 (1996).
[6] H. Tanaka, J. Phys. Condens. Matter **12**, R207 (2000).
[7] T. Koyama and H. Tanaka, Europhys. Lett. **80**, 68 002 (2007).
[8] See EPAPS Document No. E-PRLTAO-102-004909 for a supplementary movie. For more information on EPAPS, see http://www.aip.org/pubservs/epaps.html.
[9] F. Spaepen, Acta Metall. **25**, 407 (1977).
[10] A. S. Argon, Acta Metall. **27**, 47 (1979).
[11] A. E. Carsson and E. R. Fuller, Jr., *Fracture: Instability Dynamics, Scaling, and Ductile/Brittle Behavior* (Materials Research Society, Boston, 1996).
[12] M. L. Falk and J. S. Langer, Phys. Rev. E **57**, 7192 (1998).
[13] A. Furukawa and H. Tanaka, Nature (London) **443**, 434 (2006); A. Furukawa and H. Tanaka, unpublished.
[14] H. Tanaka and T. Araki, Phys. Rev. Lett. **78**, 4966 (1997).
[15] H. Tanaka, Y. Nishikawa, and T. Koyama, J. Phys. Condens. Matter **17**, L143 (2005).
[16] M. Doi and S. F. Edwards, *The Theory of Polymer Dynamics* (Clarendon Press, Oxford, 1986).
[17] R. Larson, *The Structure and Rheology of Complex Fluids* (Oxford University Press, Oxford, 1999).
[18] M. Tempel, G. Isenberg, and E. Sackmann, Phys. Rev. E **54**, 1802 (1996).
[19] D. Mizuno *et al.*, Science **315**, 370 (2007).
[20] J. Walker, Sci. Am. **255**, 204 (1986); M. Ryan and C. Sammis, Geol. Soc. Am. Bull. **89**, 1295 (1978); A. Skjeltorp and P. Meakin, Nature (London) **335**, 424 (1988).A. Groisman and E. Kaplan, Europhys. Lett. **25**, 415 (1994); K. A. Shorlin *et al.*, Phys. Rev. E **61**, 6950 (2000).